Geomechanics and Engineering, *Vol. 26, No. 1 (2021) 1-12*
https://doi.org/10.12989/gae.2021.26.1.001

Load-displacement behaviour of tapered piles: Theoretical modelling and analysis

Yunong Li*[1] and Wei Li[1,2a]

[1]*Key Laboratory of Green Construction and Intelligent Maintenance for Civil Engineering of Hebei Province, Yanshan University, Qinhuangdao, Hebei Province, People's Republic of China*
[2]*School of Civil Engineering & Mechanics, Yanshan University, Qinhuangdao, Hebei Province, People's Republic of China*

(Received December 10, 2020, Revised May 24, 2021, Accepted June 17, 2021)

Abstract. This paper presents a simplified analytical approach for evaluating the load-displacement response of single tapered pile and pile groups under static axial compressive loads. The response of the tapered pile shaft is considered elastically in the initial stage, whereas the increase in stresses due to slippage along the pile-soil interface is obtained from a developed undrained cylindrical cavity expansion solution based on the K_0-based anisotropic modified Cam-clay (K_0-AMCC) model. An effective iterative computer program is developed to calculate the load-displacement behaviour of a single tapered pile. Regarding the response analysis of tapered pile groups, a finite-difference method is employed to calculate the interaction between tapered pile shaft, and the linear elastic model to simulate the interaction developed at the pile base. A reduction coefficient is introduced into the analysis of pile shaft interaction to clarify the reinforcing effect between tapered piles. Therefore, the settlement calculation methods of pile groups are proposed for different pile cap stiffness. The calculation methods of single tapered pile and pile groups are validated using two 3D Finite Element (FE) programs, and the comparison results show that reasonable predictions can be made using the method proposed in this paper. Parametric studies are conducted to investigate the effects of taper angle, soil anisotropy, pile spacing, and pile number on the load-displacement behaviour of single tapered pile and tapered pile groups.

Keywords: cylindrical cavity expansion; K_0-AMCC model; load-displacement behaviour; single tapered pile; tapered pile groups

1. Introduction

Tapered piles, which have top cross-sections larger than the bottom ones, have the bearing capacity advantages over straight-sided cylindrical piles and also have potentially significant cost advantages in static axial load conditions. Due to these good performances, in the last three decades, increasing interest to study the behaviour of tapered piles under axial loads has been found, various experimental tests include those conducted by Wei and El Naggar (1998), El Naggar and Sakr (1999), Sakr and El Naggar (2003), Khan *et al*. (2008), Paik *et al*. (2011, 2013), Manandhar and Yasufuku (2013). Zil'berberg and Sherstenv (1990) conducted field tests of tapered and cylindrical piles driven into sandy soil, which show that the axial bearing capacity of tapered piles is 2.0-2.5 times than of cylindrical piles with the same average embedded diameter and length. Wei and El Naggar (1998) studied the load-displacement behaviour and taper effect of tapered piles by developing a series of laboratory model tests. They suggested that the taper angle should be limited to the top 20 pile diameters of the pile length for optimum efficiency. Paik *et al*. (2013) observed that the bearing capacity ratio of tapered to cylindrical piles varies with the taper angle and sand conditions. Besides, some numerical simulation studies on the load-displacement behaviour of tapered piles using Finite Element Method (FEM) have also been reported (Kurian and Srinivas 1995, Kodikara *et al*. 2006, Khan *et al.* 2008, Hataf and Shafaghat 2015). Although 3-dimensional (3D) FEM analyses are more appropriate for the numerical simulation of the load-displacement response of piles, the majority of past numerical models of tapered piles have assumed the solution domain to be two-dimensional. Kodikara *et al*. (2006) studied the numerical model of the tapered pile embedded in mudstone and found that taper has a significant advantage for an axial load capacity in comparison to cylindrical piles. Khan *et al.* (2008) established an axisymmetric finite element model and compared it with their test results to prove the beneficial effects of pile taper. Furthermore, Hataf and Shafaghat (2015) studied the relationship between different taper angles and their maximum bearing capacity using the 3D FEM and pointed out that the optimal tapering angle reaches 1.2° in dense sands.

The theoretical methods have been developed for calculating the load-displacement response of the tapered piles. Based on Mohr-Coulomb theory, Liu *et al.* (2012) derived a method to analyze the load-displacement of tapered piles, taking into account the influence of the pile-soil radial interaction. Kodikara and Moore (1993) proposed a model to calculate the side resistance of tapered piles in

*Corresponding author, Associate Professor
E-mail: yunongli@ysu.edu.cn
[a]Ph.D. Student
E-mail: 13191816153@163.com

Copyright © 2021 Techno-Press, Ltd.

ISSN: 2005-307X (Print), 2092-6219 (Online)

the cohesive-frictional ground. Three analysis stages are used in the article to express the relationship between changing shear stress and pile displacement. In the third stage, the nonlinear displacement of soil is considered based on several cavity expansion solutions. Manandhar and Yasufuku (2012, 2013) further developed the stress-dilatancy relationship to evaluate the skin friction along the tapered piles side, and to compute the end-bearing capacity of using spherical cavity expansion solution in sandy soils. Singh and Patra (2020) evaluated stresses acting at the soil-pile interface due to slippage using a cylindrical cavity expansion solution. These studies show that the cavity expansion theory is suitable for explaining the load transfer during the settlement of tapered piles.

Although there have been many studies on load-displacement analysis, most of them are aimed at analyzing tapered piles in sandy soils, with few references to tapered piles in anisotropic soft clay. Some related studies have shown that anisotropic behaviour is one of the most significant properties of soil (Li and Zou 2019, Li *et al*. 2019, Yang *et al*. 2020, 2021, Li *et al*. 2021). Considering the lack of current research on this issue, the primary objective of this paper is to propose a methodology for analyzing the load-displacement response of individual tapered piles and pile groups in anisotropic soft clay. For this, an undrained cylindrical cavity expansion solution considering the effects of the initial stress anisotropy is incorporated into the load transfer model to evaluate the radial stress acting on the soil-pile interface. The solution was originally derived by Li *et al*. (2016) based on the K_0-based Anisotropic Modified Cam-Clay (K_0-AMCC) model. An iterative computer program is developed for analyzing the load-displacement behaviour of a single tapered pile. Furthermore, in an adjacent identical tapered pile analysis system, the finite-difference method is adopted to solve the shaft response of unloaded adjacent pile, and the linear elastic model is used to simulate the interaction between pile bases. To illustrate the reinforcing effect between tapered piles, a reduction coefficient is introduced into the analysis of pile shaft interaction. A settlement analysis method then is proposed for the tapered pile groups with different pile cap stiffness. The validity of the proposed approach is examined by comparing the predicted load-displacement curves with the results obtained from the 3D FE programs. Besides, parametric studies are conducted to explore the variation of taper angle, soil anisotropy, pile spacing, and pile number on the load-displacement behaviour of single tapered pile and tapered pile groups.

2. General response of tapered pile

In this analysis, tapered piles with a circular cross-section are considered. It is assumed that the total resistance of the pile comprises shaft resistance and base resistance. The axial compressive load has been applied monotonically, and the compressive stresses and strains are taken as positive throughout the analysis.

To obtain the general response of the tapered pile, the basic differential equation of the compressible elastic pile can be established by taking a small segment of length dz at the depth of z from the tapered pile top, as shown in Fig. 1. The equilibrium equation can be expressed as

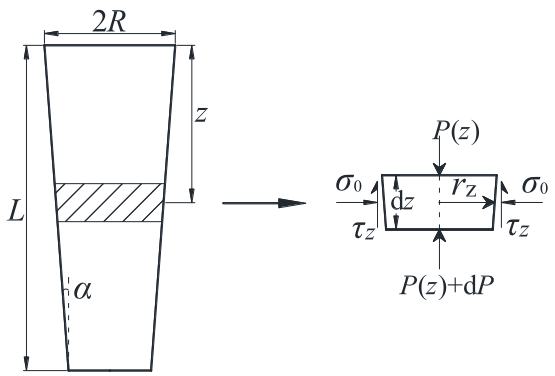

Fig. 1 Geometry of the tapered pile and a segment at a depth z from the top

$$\frac{\mathrm{d}P(z)}{\mathrm{d}z} = 2\pi r_z \tau(z) \tag{1}$$

where at the depth z, $P(z)$ = axial force acting on the top of small segment dz, $\tau(z)$ = vertical component of the shear stress acting along the pile-soil interface and r_z = pile radius, r_z=R-$z$tanα; R and α = pile head radius and taper angle of the tapered pile, respectively. In order to achieve the requirement that the vertical component ($\tau(z)$= $\tau_0$cosα) is almost equal to the shear stress along the pile-soil interface (τ_0), the taper angle value should be less than 5°.

According to Hooke's law, the relationship between the axial strain and the axial load of the pile is as follows

$$\frac{\mathrm{d}W(z)}{dz} = \frac{P(z)}{E_p A_z} \tag{2}$$

where $W(z)$ = pile displacement, A_z = cross-sectional area of the section (πr_z^2) and E_p = Young's modulus of the pile material. Combining Eqs. (1) and (2), the governing differential equation for pile-soil interaction can be obtained, as follows

$$E_p A_z \frac{\mathrm{d}^2 W(z)}{\mathrm{d}z^2} + E_p \frac{\mathrm{d}A_z}{\mathrm{d}z} \cdot \frac{\mathrm{d}W(z)}{\mathrm{d}z} - 2\pi r_z \tau(z) = 0 \tag{3}$$

If the τ-W relationship is known, this differential equation can be solved through any numerical technique like the finite element method, finite difference, or approximate methods such as the segment-by-segment approach or load transfer method (Singh and Patra 2020).

3. Calculation model of a single tapered pile

Various τ-W transfer relationships have been proposed for axially loaded cylindrical piles in previous studies, such as the hyperbolic nonlinear model (Zhang and Zhang 2012) and BoxLucas1 exponential model (Wang *et al.* 2012, Li *et al.* 2017a, 2020). These empirical models obtained from the experimental results believe that there is a limit shear stress on the pile shaft, so that the pile displacement can increase indefinitely after reaching the shear stress limit. However,

in contrast to the cylindrical pile, the tapered pile has a variable cross-section, the shear stress keeps increasing with the pile displacement due to the additional radial expansion of the ground caused by the pile shaft. Therefore, taking into account the characteristics of this aspect, the load transfer relationships of the tapered piles are specifically analyzed, and the shaft resistance and base resistance models are described below.

3.1 Shaft resistance

The analysis of shaft resistance is considered as three phases, of which the first phase assumes that the pile and the surrounding soil are elastically deformed and there is no slippage. In the second and third phases, slippage occurs at the pile-soil interface and the surrounding soil produces expansion displacement. The elastic and elastoplastic solutions of cylindrical cavity expansion theory can be used to analyze the expansion pressure caused by slip.

3.1.1 In Phase Ⅰ

This phase is similar to a cylindrical pile undergoing initial elastic deformation. The vertical displacement of surrounding soil, $W_{se}(z)$, induced by the axial shear stresses $\tau(z)$, can be approximately expressed by the elastic solution proposed by Randolph and Wroth (1978):

$$W_{se}(z)=\frac{r_z}{G_s}\tau(z)\ln\left(\frac{r_m}{r_z}\right) \tag{4}$$

where G_s = shear modulus of the soil around the pile shaft, and r_m = the influence range of the surrounding soil settlement caused by the pile displacement at a given depth z, i.e., the maximum radial distance from the pile center to affected soil. In homogeneous soil, r_m can be calculated by the formula suggested by Randolph and Wroth (1978) as

$$r_m=2.5L(1-0.5\nu_s) \tag{5}$$

where L = pile length and ν_s= value of Poisson's ratio in the soil. In arbitrarily layered soils, a modified expression was suggested by Lee (1993) as follows

$$r_m=2.5L\rho_m(1-\nu_m) \tag{6}$$

where ρ_m = modified inhomogeneity factor, $\rho_m=(\sum_{k=1}^{m_s}G_{sk}L_k)/(G_{sm}L)$; ν_m = average value of Poisson's ratio in the soil, G_{sm} = maximum shear modulus in the soil layers, G_{sk} = shear modulus of soil layer k, L_k = pile length placing in soil layer k, and m_s = number of soil layers.

Since the displacement of the pile (W_{ce}) and the surrounding soil are the same at this phase (i.e., $W_{se}=W_{ce}$), the reasonable τ-W relationship is

$$\tau(z)=\frac{W_{ce}(z)G_s}{r_z\ln(r_m/r_z)} \tag{7}$$

This phase will continue until the soil reaches yield at the pile-soil interface. Consider the small section of the pile shown in Fig. 1, the shear stress when the interface yields can be expressed as

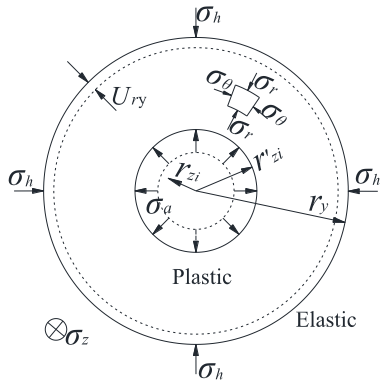

Fig. 2 Mechanical model for cylindrical cavity expansion

$$\tau_{z0}=\sigma_0'\tan(\alpha+\delta)+\frac{c\sec^2\alpha}{1-\tan\alpha\tan\delta} \tag{8}$$

where σ_0' = initial horizontal stress of the surrounding soil, $\sigma_0'=K_0\gamma_s'z$, z = depth from the ground to the midpoint of the analysis segment, γ_s' = unit mean effective weight of the soil above depth z; K_0 = coefficient of the lateral earth pressure and the values of K_0 are estimated by the empirical formula suggested by Manyne and Kulhawy (1982), $K_0=(1-\sin\varphi')\mathrm{OCR}^{\sin\varphi'}$, OCR = over-consolidation ratio of the soil; δ = the friction angle at the pile-soil interface, $\delta=\varphi'/3$, φ' = friction angle of the surrounding soil; and c = cohesion at the pile-soil interface.

3.1.2 In Phase Ⅱ

In the second and third phases, slip occurs at the pile-soil interface and the vertical pile movement at any point on the pile-soil interface is greater than the soil movement at the corresponding point on the interface. The vertical displacement of the tapered pile can be monitored by the radial expansion, when the vertical pile moves W_c, the radial expands from the initial radius r_z to the current radius r_z' at any horizontal layer. According to simple geometric relations, the current pile radius r_z' can be expressed as follows

$$r_z'=R-(z-W_c)\tan\alpha \tag{9}$$

This radial expansion mechanism is extremely consistent with the cavity expansion theory, as shown in Fig. 2. Therefore, an elastoplastic solution of the undrained cylindrical cavity expansion based K_0-AMCC model is used to describe the increased radial deformation and confining stress of the surrounding soil (Li *et al*. 2016). Considering the in-situ anisotropic stress state, the relationship between the in-situ effective horizontal stress, σ_{r0}', the effective circumferential stress, $\sigma_{\theta0}'$, the effective vertical stress, σ_{z0}', and initial pore water pressure, u_0, at the surrounding soil is as follows

$$\sigma_{r0}'=\sigma_{\theta0}'=(\sigma_{h0}-u_0)=K_0\sigma_{z0}' \tag{10}$$

When the vertical pile movement is small, the soil

around the pile is in an elastic state. The effective stress and radial displacement of the soil around the pile shaft can be described by elastic solution of cavity expansion theory, as follows

$$\sigma_r' = \sigma_{h0}' + \left(\sigma_{rp}' - \sigma_{h0}'\right)\left(\frac{r_p}{r}\right)^2 \tag{11}$$

$$\sigma_\theta' = \sigma_{h0}' - \left(\sigma_{rp}' - \sigma_{h0}'\right)\left(\frac{r_p}{r}\right)^2 \tag{12}$$

$$U_r = \frac{\sigma_{rp}' - \sigma_{h0}'}{2G_s}\left(\frac{r_p}{r}\right)^2 r \tag{13}$$

where σ_r' and σ_θ' = effective radial and tangential stresses, respectively. The expressions of the shear modulus G_s, the effective radial stress σ_{rp}' at the elastic-plastic boundary and the plastic radius r_p, respectively, as follows

$$G_s = \frac{3(1-2\nu_s)\upsilon p'}{2(1+\nu_s)\kappa} \tag{14}$$

$$\sigma_{rp}' = \sigma_{h0}' + \frac{1}{\sqrt{3}} p_0' \eta_p^* \tag{15}$$

$$\left(\frac{r_p}{r_z'}\right)^2 = \frac{1}{1-\left(\frac{\sigma_{rp}' - \sigma_{h0}'}{2G_s} - 1\right)^2}\left(1 - \frac{r_z^2}{r_z'^2}\right) \tag{16}$$

where υ = specific volume, $\upsilon = 1+e$, e = void ratio of soil; κ = slope of the loading-reloading line in the $\upsilon - \ln p'$ plane; p' = mean effective stress, $p' = (\sigma_r' + \sigma_\theta' + \sigma_z')/3$, and $p_0' = [(1+2K_0)\sigma_{z0}']/3$. The relative stress ratio at the elastic-plastic boundary η_p^* can be expressed as

$$\eta_p^* = M^* \sqrt{\mathrm{OCR} - 1} \tag{17}$$

where M^* = relative stress ratio at the critical state, $M^* = \sqrt{M^2 - \eta_0^2}$; M = slope of the critical state line, $M = 6\sin\varphi'/(3-\sin\varphi')$; η_0 = in situ stress ratio, $\eta_0 = \left|3(1-K_0)\right|/(2K_0+1)$.

According to Eqs. (9) and (15), the effective radial stress at the pile wall σ_a' in the elastic stage, can be obtained as

$$\sigma_a' = \sigma_{h0}' + \frac{1}{\sqrt{3}} p_0' \eta_p^* \left(\frac{r_p}{r_z'}\right)^2 \tag{18}$$

Therefore, the τ-W relationship is obtained by transforming the stress at the pile wall, as follows

$$\tau_z = \sigma_a' \tan(\alpha + \delta) + \frac{c\sec^2\alpha}{1 - \tan\alpha\tan\delta} \tag{19}$$

3.1.3 In Phase Ⅲ

As the pile displacement and internal pressure further increase, there will come a stage when the soil immediately adjacent to the cavity wall begins to yield from an elastic stage to a plastic state. Using the aforementioned equations, the critical displacement value of the tapered pile W_p can be expressed as

$$W_p = W_{se} + \Delta W_p \tag{20}$$

By substituting Eqs. (15) and (18) into Eq. (13), the settlement increment of the soils surrounding the pile shaft ΔW_p ($0° < \alpha < 5°$) can be obtained as

$$\Delta W_p = \frac{(R - z\tan\alpha)\, p_0' \eta_p^*}{(2\sqrt{3}G_s - p_0'\eta_p^*)\tan\alpha} \tag{21}$$

After the initial yielding at the cavity wall, a zone of soil extending from the cavity wall to a radial distance r_p will become plastic as the cavity pressure continues to increase. In the plastic stage, the total radial stress σ_a and excess pore pressure Δu_a at the pile wall were derived by Li *et al.* (2016), as follows

$$\sigma_a = \sigma_{h0} + \frac{1}{\sqrt{3}} p_0' \eta_p^* + \frac{\xi p_f'}{2} \ln \frac{G_s}{(\sigma_{rp}' - \sigma_{h0}')}\left(1 - \frac{r_z^2}{r_z'^2}\right) \tag{22}$$

$$\Delta u_a = \sigma_{h0}' + \frac{1}{\sqrt{3}} p_0' \eta_p^* - p_f' + \frac{\xi p_f'}{2}\left[\ln \frac{G_s}{(\sigma_{rp}' - \sigma_{h0}')}\left(1 - \frac{r_z^2}{r_z'^2}\right) - 1\right] \pm \frac{\sqrt{4M^2 - 3\xi^2}}{6} \tag{23}$$

where the plus sign is taken when $K_0 \le 1$; conversely, the minus sign is taken when $K_0 > 1$. The ultimate mean stress p_f' in the soil adjacent to the pile, and the parameter ξ can be given, respectively, as follows

$$p_f' = p_0'\left(\frac{\mathrm{OCR}}{2}\right)^{\Lambda} \tag{24}$$

$$\xi = \frac{2\sqrt{3[M^2(2K_0+1)^2 - 9(1-K_0)^2]}}{3(2K_0+1)} \tag{25}$$

where Λ is the plastic volumetric strain ratio, $\Lambda = 1 - \kappa/\lambda$, where κ and λ are the slopes of the swelling line and the loading line, respectively.

During the settlement of the tapered pile, the relative slip between the pile shaft and the soil above the pile end is a sliding friction, and the effective expansion pressure should be used to calculate the sliding friction resistance of the pile side. According to Eqs. (22)-(23), the effective radial expansion stress at the pile wall, σ_a', can be obtained as

$$\sigma_a' = \sigma_a - (u_0 + \Delta u_a) = \frac{(\xi+2)p_f'}{2} \mp \frac{\sqrt{4M^2 - 3\xi^2}}{6} \tag{26}$$

Finally, by substituting Eq. (26) into Eq. (19), the τ-W relationship of the plastic stage can be obtained.

3.2 Base resistance

The general bearing characteristics of the tapered pile

are the combination of friction and end-bearing pile. Results from the load tests on instrumented piles (Khan *et al.* 2008) indicated that 76% of the capacity is due to shaft resistance and only 24% is due to base capacity. He *et al.* (2012) also pointed out that the end resistance of the tapered pile is 3%-15% of the load on the top. For the small pile base resistance, it is reasonable to apply this elastic model to calculate. Therefore, the pile base settlement is estimated by the solution of a rigid punch acting on an elastic half-space soil, as suggested by Randolph and Wroth (1978). Hence, the relationship between mobilized pile base load (P_b) and pile base settlement (W_b) is expressed as

$$W_b = \frac{P_b(1-\nu_{bs})\omega}{4r_0 G_{bs}} \tag{27}$$

where G_{bs} = shear modulus, ν_{bs} = Poisson's ratio of the pile base soil, r_0 = pile radius at the base, ω = a coefficient used to account for the effect of the depth of the pile tip below the surface, and its range is approximately from 1.1 to 1.7 (Guo and Randolph, 1998).

3.3 Algorithm for load-displacement behaviour of a single tapered pile

To obtain an effective and accurate solution, a single tapered pile can be divided into n segments, which are rigidly connected, as shown in Fig. 3. When the number of segments is large, it is assumed that the load in the segments varies linearly, and the following procedure can be adopted:

(1) Assume a small pile end settlement W_{bn}.

(2) Calculate the pile base load, P_{bn}, corresponding to the deformation W_{bn}, using Eq. (27).

(3) A vertical movement, W_{cn}, at the middle height of pile segment n is assumed (for the first trial, assume W_{cn} = W_{bn}).

(4) Take the nth segment analysis as an example, estimate the unit shaft resistance τ_{zn} at the midpoint of the segment n, using the estimate of midpoint displacement W_{cn} as follows:

a. if $W_{cn} < W_{se}$, then estimate τ_{zn} from Eq. (7),

b. if $W_{se} < W_{cn} < W_p$, then estimate τ_{zn} from Eqs. (18) and (19),

c. if $W_{cn} \geq W_p$, then estimate τ_{zn} from Eqs. (26) and (19),

(5) The load on the top of the tapered pile segment n, P_{tn}, can be calculated from the following

$$P_{tn} = P_{bn} + 2\pi(R - z_n \tan\alpha)L_n\tau_{zn} \tag{28}$$

where L_n = length of pile segment n; P_{bn} = the load on the bottom of the pile segment n.

(6) Calculate the elastic deformation in the midpoint of the segment n (assuming a linear variation of load in the segment) by

$$W'_{cn} = W_{bn} + \left(\frac{P_{tn} + 3P_{bn}}{4}\right)\left[\frac{L_n}{2\pi(R - z_n \tan\alpha)^2 E_p}\right] \tag{29}$$

Compare the updated midpoint displacement W'_{cn} with the assumed value of W_{cn} from step 3. If the calculated displacement W'_{cn} does not agree with W_{cn} within a specified tolerance, e.g., 1×10^{-6} m, set $W_{cn} = W'_{cn}$. Then repeat steps 4-6 until the value of $|W'_{cn}-W_{cn}|$ is within the assumed tolerance.

(7) Calculate the load and displacement at the top of pile segment n, P_{tn} and W_{tn}, respectively, using the following equations

$$P_{tn} = P_{bn} + 2\pi(R - z_n \tan\alpha)L_n\tau'_{zn} \tag{30}$$

$$W_{tn} = W_{bn} + \left(\frac{P_{tn} + P_{bn}}{2}\right)\left[\frac{L_n}{\pi(R - z_n \tan\alpha)^2 E_p}\right] \tag{31}$$

where τ'_{zn} is derived from sept 4 and an updated midpoint displacement W'_{cn}.

(8) The bottom settlement of pile segment (i-1) is taken as the top settlement of pile segment i (i = 2, 3, 4, ..., n)

$$W_{b(i-1)} = W_{ti},\ P_{b(i-1)} = P_{ti}, (i = 2,3,\cdots,n) \tag{32}$$

(9) Repeat steps 3-8 from pile segment n to pile segment 1 until the load-displacement relationship developed at the pile head is obtained.

(10) The procedure from steps 1-9 is then repeated using gradually increasing assumed pile end settlement W_{bn} until a series of load-displacement values are obtained.

According to the above process, a computer code based on MATLAB software is developed to capture the bearing performance of the pile top. The present analytical approach only requires a few seconds to predict the load-displacement curve of a tapered pile, which demonstrates the present approach is quite economical and efficient.

4. Analysis of pile-soil-pile group interaction

The pile group system consists of m single tapered piles with length L. Consider a pair of identical tapered piles, i and j, as shown in Fig. 4. It is assumed that the superposition principle applies to the analysis of the interaction between two identical piles. The pile-soil-pile interaction is considered as linear elasticity, and the load pile is nonlinear in this study (Wang *et al.* 2012). Therefore, the total settlement of pile i, $S_{i,z}$, can be written as the sum of the settlement due to its loading plus any additional settlement caused by the interaction of adjacent piles along the pile shaft and pile base. It can be expressed as follows at the depth z,

$$S_{i,z} = W_{ii,z} + W_{\mathrm{sei}j,z} + W_{\mathrm{bi}j,z} \tag{33}$$

where $W_{ii,z}$ = displacement of pile i induced by its axial load, and $W_{seij,z}$ = additional elastic displacement induced by the shaft stresses of pile j. $W_{bij,z}$ = additional pile base displacement induced by pile j.

4.1 Interaction between tapered pile shafts

In order to analyze the load pile displacement caused by adjacent unloaded pile shaft, the pile shaft interaction factor ς_s originally proposed by Mylonakis and Gazetas (1998) is employed, and its expression is as follows

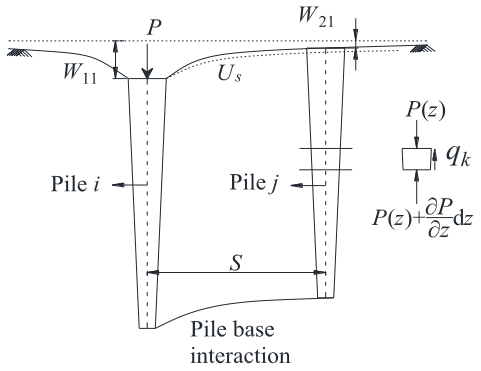

Fig. 4 Pile-soil-pile interaction between two identical tapered piles

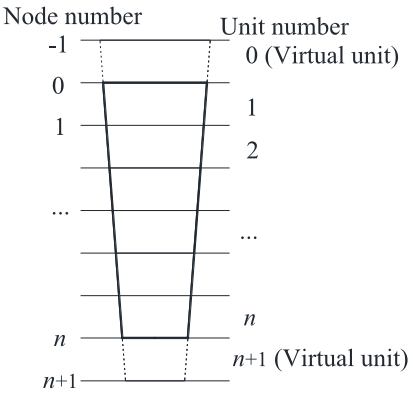

Fig. 5 Difference units of single tapered pile

$$\varsigma_s = \begin{cases} \dfrac{\ln(r_m)-\ln(s)}{\ln(r_m)-\ln(r_z)} & \dfrac{r_z}{2} \le s \le r_m \\ 0 & s \ge r_m \end{cases} \tag{34}$$

where s = center-to-center distance between two identical piles, r_m = limit influence radius of the pile, and its range is considered to be consistent with the individual pile given above. Outside r_m, pile interaction is ignored (Lee and Xiao 2001).

Regardless of the effect of the unloaded pile on the settlement of the loaded pile, for any loaded pile i bearing its load, the free displacement field of the surrounding soil at the depth z, $U_s(s,z)$, can be obtained

$$U_s(s,z) = \begin{cases} \dfrac{\ln(r_m)-\ln(s)}{\ln(r_m)-\ln(r_z)} W_{11}\left(\dfrac{r_z}{2}, z\right) & \dfrac{r_z}{2} \le s \le r_m \\ 0 & s \ge r_m \end{cases} \tag{35}$$

where $W_{11}(r_z/2, z) = W_{ii,z}$.

The presence of unloaded pile j generally generates the opposite load transfer process and reduces the above displacement. Therefore, assuming that the actual settlement of the pile j at the depth z is $W_{21}(z)$, then the pile-soil relative settlement is $W_{21}(z) - U_s(s,z)$.

For an unloaded tapered pile, it can be discretized into n approximately cylindrical segments. The vertical force equilibrium can be obtained by analyzing the kth (for k = 1, 2, 3, ..., n) segment pile, as shown in Fig. 4, and expressed as

$$\frac{\partial P_k(z)}{\partial z} \mathrm{d}z + q_k = 0 \tag{36}$$

where $P_k(z)$ = pressure on the top of the kth segment, q_k = shaft resistance of the unloaded pile, $q_k = -K_{zk}\left[W_{21}(z) - U_s(s,z)\right]$; K_{zk} = shear stiffness of pile-soil interface, $K_{zk} = 2\pi G_s / \ln(r_{mk}/r_{zk})$.

According to the elastic compression of the pile, the load on the top surface of the segment can be expressed as

$$P_k(z) = E_p A_{pk} \frac{\partial W_{21}(z)}{\partial z} \tag{37}$$

where E_p = Young's modulus and A_{pk} = average cross-sectional area of the kth segment.

By substituting Eq. (37) into Eq. (36), the governing differential equation of the unloaded tapered pile considering the pile-soil-pile interaction can be transformed into the following

$$E_{pk} A_{pk} \frac{\partial^2 W_{21}(z)}{\partial z^2} - K_{zk}\left[W_{21}(z) - U_s(s,z)\right] = 0 \tag{38}$$

Since the cross-sectional area of the tapered pile is related to the location of the cross-section, Eq. (38) has no analytical solution. In the current study, the Finite Difference Method (FDM) is used, which allows easy to solve linear and nonlinear partial differential equations. The central difference rule is employed to derive the differential form of the governing differential Eq. (38). The differential form of each derivative for kth segment is as follows

$$\begin{cases} \left.\dfrac{\partial W}{\partial z}\right|_{z_k} = \dfrac{W_{k+1} - W_{k-1}}{2l} \\ \left.\dfrac{\partial^2 W}{\partial z^2}\right|_{z_k} = \dfrac{W_{k+1} - 2W_k + W_{k-1}}{l^2} \end{cases} \text{where } l = \frac{L}{n},\ k = 0,1,\cdots,n \tag{39}$$

As shown in Fig. 5, one virtual pile unit is added to the top of the unloaded pile and the end of the pile respectively, and then n+2 discrete pile units and n+3 discrete nodes are obtained. The settlement of soil around the loaded pile U_{sk} (for k = 0, 1, 2, ..., n) of n+1 real node can be obtained by using Eq. (35). By substituting Eq. (39) into Eq. (38), the difference expression of the governing differential equation of the pile element can be obtained as follows

$$\frac{1}{l^2}(W_{k+1} + W_{k-1}) - \left(\frac{2}{l^2} + \frac{K_{zk}}{E_p A_{pk}}\right) W_k = -\frac{K_{zk} U_{sk}}{E_p A_{pk}},\ k = 0,1,\cdots,n \tag{40}$$

Consider the boundary conditions of the unloaded piles, and transform them into the finite difference form as follows

$$P_0 = 0, \quad P_n = \frac{4G_{bs} r_0}{1 - \nu_{bs}} W_n \tag{41}$$

$$\begin{cases} \dfrac{E_p A_{p0}}{2l}(W_1 - W_{-1}) = 0 \\ \dfrac{E_p A_{pn}}{2l}(W_{n+1} - W_{n-1}) - \dfrac{4G_{bs} r_0}{1 - \nu_{bs}} W_n = 0 \end{cases} \tag{42}$$

Combining Eqs. (40) and (42), expressed as the

following matrix equation

$$[K_{ji}]\cdot\{W_{ji}\}=\{U_{ji}\} \tag{43}$$

where $[K_{ji}]$ is the (n+3)×(n+3) transfer matrix between pile i and pile j, $\{W_{ji}\}$and $\{U_{ji}\}$ are (n+3) vector of the settlement of unloaded pile j and the soil settlement caused by load pile i, respectively. By solving the above linear equation matrix, the elastic settlement of each segment of the unloaded pile $W_{ji}(z)$ can be obtained.

Therefore, the shaft interaction factor between two identical piles, ς_{sij}, can also be defined as the additional elastic settlement of the soil around pile i at the depth z due to the loaded adjacent pile j, divided by the elastic settlement of the soil around pile j under its load.

$$\varsigma_{sij}=\frac{W_{ij}(z)}{W_{jj}(z)} \tag{44}$$

Besides, the settlement of the unloaded pile j induces its pile-soil interface shear stress τ, which will generate a new settlement field at the surrounding soil from pile j to pile i. And the shear stress $\tau(z)$ at a depth z can be written as

$$\tau(z)=\frac{q_k}{2\pi r_z}=\frac{G_s}{r_z\ln(r_m/r_z)}[W_{21}(z)-U_s(s,z)] \tag{45}$$

According to the shear displacement theory proposed by Randolph and Wroth (1978), the settlement of load pile i caused by the shear stress $\tau(z)$, $W_{12}(z)$, is given as

$$W_{12}(z)=\frac{r_z}{G_s}\ln\left(\frac{r_m}{s}\right)\tau(z) \tag{46}$$

Substituting Eq. (45) into Eq. (46), $W_{12}(z)$ can be expressed as

$$W_{12}(z)=[W_{21}(z)-U_s(s,z)]\frac{\ln(r_m)-\ln(s)}{\ln(r_m)-\ln(r_z)} \tag{47}$$

Considering the interaction of adjacent pile j, the settlement reduction coefficient λ_{12} is defined as follows

$$\lambda_{12}=\frac{|W_{12}(z)|}{W_{11}(z)}=\begin{cases}\dfrac{U_s(s,z)-W_{21}(z)}{W_{11}(z)}\dfrac{\ln(r_m)-\ln(s)}{\ln(r_m)-\ln(r_z)} & \dfrac{r_z}{2}\le s\le r_m\\ 0 & s\ge r_m\end{cases} \tag{47}$$

4.2 Interaction between tapered pile bases

In this paper, the pile shaft and pile base interactions of individual tapered piles are considered in a pile group, separately. When the tapered pile is embedded in the soil, a displacement field can be generated under the pile base, and interactions will develop between pile bases. At a certain distance from the pile base, the load will be displayed as a point load. The settlement near a point load decreases inversely with the center distance between two identical piles. Therefore, the pile base interaction in pile groups adopts a linear elastic model, given by Randolph and Wroth (1979)

$$\varsigma_{bij}=\frac{2r_0}{\pi s_{ij}} \tag{49}$$

$$W_{bij}=W_{bjj}\varsigma_{bij}=\frac{P_{bn}(1-\nu_{bs})}{2\pi s_{ij}G_{bs}} \tag{50}$$

The top settlement of pile i in two identical pile systems can be written as the sum of the shaft settlement and the base settlement considering the interaction of pile j in the following form

$$S_i(0)=(1-\lambda_{ij})W_{ii}(0)+\varsigma_{sij}W_{jj}(0)+\varsigma_{bij}W_{bjj} \tag{51}$$

5. Settlement calculation method of tapered pile groups

According to the settlement analysis of two identical piles discussed above, in a pile group composed of m piles, the settlement correction coefficient β_i considering the effect of the interaction of adjacent piles can be expressed as follows

$$\beta_i=\prod_{j=1,\ j\neq i}^{m}(1-\lambda_{ij}),\quad i=1,2,\cdots,m \tag{52}$$

Therefore, the settlement of each tapered pile can be considered as the superposition of (m-1) pairs of two-pile system, the expression is given by

$$S_i(z)=\beta_i W_{ii}(z)+\sum_{j=1,\ j\neq i}^{m}\varsigma_{sij}W_{jj}(z)+\sum_{j=1,\ j\neq i}^{m}\varsigma_{bij}W_{bjj},\quad i=1,2,\cdots,m \tag{53}$$

When tapered pile groups with the perfectly rigid pile cap embedded in the ground surface, the top settlement of each pile is assumed to be completely consistent, and the total load acted on the pile cap, Q, is completely supported by the piles. The load and settlement of each pile can be expressed in the following form

$$\begin{cases}P_{1t}+P_{2t}+\cdots+P_{it}+\cdots+P_{mt}=Q\\ S_1(0)=S_2(0)=\cdots=S_i(0)=\cdots=S_m(0)\end{cases} \tag{54}$$

where P_{it} is the load acted on the top of pile i, and the top settlement of each pile $S_i(0)$ has the same value.

When tapered pile groups with perfectly rigid pile cap embedded beneath the ground surface, the subsoil under the pile caps may share a part of the top load. But it is difficult to determine the proportion of the actual load shared by the subsoil. Even in soft soil areas, the pile cap may not contact the subsoil due to its consolidation settlement. Therefore, the relationship between the settlement and a load of each pile can also be predicted using Eq. (54). Whereas for a group of m piles with a perfectly flexible cap, the load shared by each pile is considered as identical; that is, $P_{it}=Q/m$, and the settlement of each pile can be evaluated using Eq. (53).

6. Verification of proposed method

To assess the performance of the proposed calculation models in predicting the settlement of tapered piles, the comparison with reliable in-situ data from available literature is most appropriate. However, there is a dearth of

Table 1 Mechanical properties of silty clay

Soil property	Value
Effective unit weight [γ' (kN/m^3)]	8.0
Effective internal friction angle [φ' (degree)]	31.7
Slope of loading line (λ)	0.11
Slope of swelling line (κ)	0.021
Void ratio (e_0)	1.5
Earth pressure coefficient at rest (K_0)	0.55
OCR	1.0
Poisson's ratio (v_s)	0.33
Coefficient of permeability [k (m/s)]	2×10^{-6}

(a) Single tapered pile model (b) Tapered pile group model

Fig. 6 Three-dimensional finite element meshes

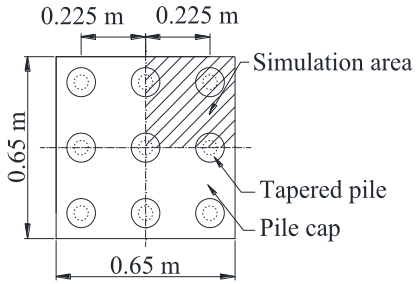

Fig. 7 Layout of the tapered pile group

case studies on the in-situ parameters of cohesive soil consistent with the K_0-AMCC model. On the other hand, 3D FEM is considered one of the most powerful approaches for the analysis of single piles and pile groups under axial compressive loads (Comodromos *et al*. 2009, Hamderi 2018). This method uses more input parameters and an environment closer to real engineering, which improves the reliability of the simulation results. Therefore, in this study, two 3D FE programs are applied to verify the load-displacement behaviour of a single tapered pile and a group of tapered piles, respectively, taking into account the anisotropic characteristics of soft clay. In order to ensure the accuracy and rationality of the comparison results, in all numerical analyses performed, it is assumed that the material properties of clay and tapered piles and the pile-soil interface parameters are consistent with the proposed calculation models.

Finite element analyses were performed using the program ABAQUS. Regardless of whether in a single pile or a pile group system, since the effective influence zone has two symmetry planes, it is only necessary to numerically simulate the behaviour of the system over a quarter of the domain. Fig. 6(a) shows the finite element mesh of a single tapered pile in the soft clay foundation. The length of the tapered pile L = 1.2 m, the pile head radius R= 50 mm, and the pile tip radius r_0 = 25 mm, and then the taper angle α = 1.19°. The soft clay was assumed to be normally consolidated silty clay and was modeled as a modified Cam clay material. The basic characteristic parameters of the silty clay related to the model were given according to the test results of Li *et al.* (2020) and were summarized in Table 1. The tapered pile was modeled using a linear elastic model with a Poisson's ratio v = 0.2 and an elastic modulus E_p = 22 GPa (e.g., Liu *et al*. 2010). A Mohr-Coulomb failure criterion was used for the interface elements, the interface friction angle φ' = 31.7° and the cohesion at the soil-pile interface c = 3.5 kPa. The coefficient of sliding friction (μ) between the soil and pile was selected to be 0.4 (μ = 2/3tanφ'; Elias *et al*. 2006). Note that the permeability coefficient and sliding friction coefficient are not required in the proposed model. In the process of simulating settlement, the top surface units of the pile were subjected to a series of vertical downward displacements. As vertical displacement increases, the resultant stress is recorded, allowing the load-displacement curve to be drawn accordingly.

Moreover, in order to check the reliability of the proposed method for analyzing the load-displacement behaviour of tapered pile groups, a nine-pile group is

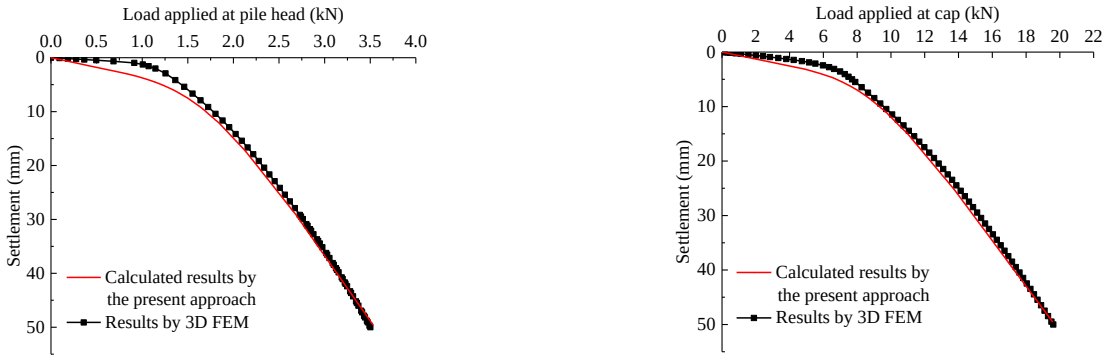

(a) Single tapered pile (b) Tapered pile group

Fig. 8 Comparison of load-displacement between the simulation and computed results

installed in a 3×3 configuration with a center-to-center spacing of s = 4.5R, and the layout plan of the pile group top is shown in Fig. 7. The simulation of a quarter model of the tapered pile group is also established as shown in Fig. 6(b). The parameters of tapered piles and surrounding soil are the same as above, and the cap for the pile group was given a large stiffness to ensure that it was rigid and hence behaved as observed on site. The rigid cap and the pile tops are tied together, assuming no slip on the contact surface during load application. Furthermore, the pile cap is slightly higher than the top surface of the soil, and will not touch it during the settlement process, ensuring that the applied load is fully shared by the piles.

Fig. 8(a) shows the load-displacement response of both the proposed analytical calculation method and the 3D FEM with the same input parameters. It is observed that the predicted results are in good agreement with the numerical simulation results. As seen in Fig. 8(a), the top settlement of a single tapered pile is shown as an initial linear segment followed by a significant increase in settlement corresponding to a disproportionate increase in the load. However, the settlements obtained by the calculation method increase faster in the initial load stage, which may be because the values of the cohesive force account for a larger proportion in the load transfer at this stage. Both curves have almost the same performance after the load increases, which demonstrates that load-displacement behaviour can be properly predicted by the elastic solution and elastoplastic solution of anisotropic cavity expansion theory, respectively. Besides, it is interesting to note that the load-bearing capacity of the tapered pile keeps increasing with the increase in applied load, and no limiting value is observed within the pile head displacement of 50 mm. Because of the taper angle effect, the surrounding soil has been radially expanded during the settlement process, resulting in a significant increase in the bearing capacity of the tapered pile, unlike the equal-diameter pile recorded by Li *et al.* (2017b) that the load hardly increases after the soil yields.

Fig. 8(b) presents the comparison between the proposed method results and the simulation results. It can be seen that the predicted curve matches closely with the simulation curve, which suggests that the proposed analytical approach can be applied to evaluate the load-displacement response for tapered pile groups. Meanwhile, the settlement trend of the pile group is observed to be similar to the results of the single pile, but this does not mean that the settlement of pile group is superimposition by the single pile load according to the quantity. This is because in the settlement process in the natural clay, accompanied by the rise of excess pore pressure and slight ground floatation, the bearing capacity is reduced relative to the sum of the single piles.

7. Parametric analysis

In this section, parametric analyses are conducted to show the load-displacement response of an individual tapered pile and tapered pile groups. The responses investigated include the influence of taper angle and lateral earth pressure coefficient for an individual tapered pile, and the influence of pile spacing and pile number for tapered pile groups. The soil parameters used here are the same as those listed in Table 1. The corresponding analysis results are displayed in Figs. 9 and 10.

7.1 Influence of taper angle and lateral earth pressure coefficient

To investigate the taper angle effect, four tapered piles with the same material and length, as shown in Table 2, are analyzed. The load-displacement response analysis for an individual tapered pile is shown in Fig. 9. It can be observed from Fig. 9(a) that with an increase in the taper angle (small angles up to 1.8°), the settlement under the same load decreases but the effect is insignificant in the initial elastic stage. Moreover, it should be noted that the load at the inflection point also increases with the increase of the taper angle. As the load increases after the inflection point, the settlement rate is larger, the settlement curve steepening.

The anisotropy of surrounding soil is reflected by different coefficients of the lateral earth pressure. As shown in Fig. 9(b), the lateral earth pressure coefficients K_0 = 0.55, 0.70, 0.85 and 0.99 are adopted to analyze the load-displacement response of the T3 tapered pile. It is found that the settlements decrease significantly with the increase of the lateral earth pressure coefficient (i.e., the soil is gradually approaching isotropy). Without considering the anisotropy of the surrounding soil, the predicted bearing performance of the tapered pile is larger than the actual situation. For example, when the tapered pile settlement is

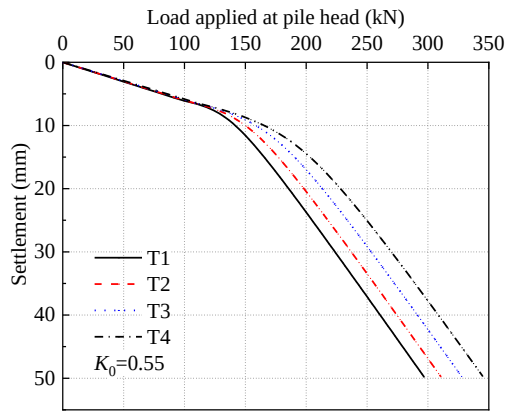

(a) The influence of different taper angles

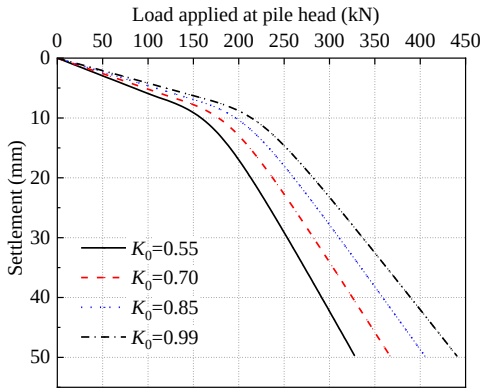

(b) The influence of lateral earth pressure coefficients

Fig. 9 Variation of load-displacement curves of the single tapered pile

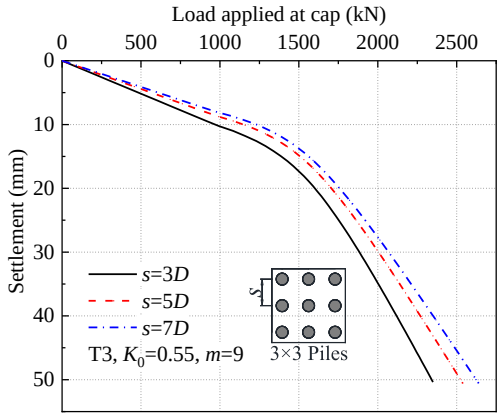

(a) The influence of different pile spaces

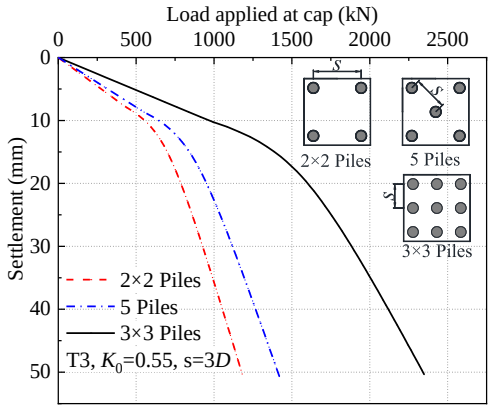

(b) The influence of different pile numbers

Fig. 10 Variation of load-displacement curves of the tapered pile groups

Table 2 The properties of tapered piles used in parameter study

Pile name	R (mm)	r_0 (mm)	α (degree)	L (m)	D^*(mm)
T1	314	300	0.1	8	614
T2	384	300	0.6	8	684
T3	468	300	1.2	8	768
T4	551	300	1.8	8	851

*D: The Average Diameter of Tapered Pile

50 mm, the load-bearing capacity of the pile with the lateral earth pressure coefficients of 0.85, 0.70 and 0.55 are reduced by 8.1%, 16.8% and 25.6% compared with the case in isotropic soil, respectively.

7.2 Influence of pile spacing and pile number

Fig.10(a) and 10(b) plot the load-displacement curves of different pile spacing and pile number in the pile groups. The load range of the horizontal axis refers to the load acting on the top of the rigid pile cap. Since the rigid pile cap hardly touches the soil underneath, the load is almost completely shared by the pile. As shown in Fig. 10(a), the settlement of the pile top decreases with the increase of the pile spacing under the same load. This is because the pile-pile interaction decreases as the area of soil covered under the pile cap increases, which also leads to the weakening of the pile group effect and showing the bearing performance of more individual piles. Furthermore, it is also interesting to see from Fig. 10(a) the trend of settlement is almost unchanged with the increase of pile spacing. There are obvious inflection points in the settlement process, and the settlement rate increases after reaching the ultimate bearing capacity, but the decline is not sharp due to the influence of the taper angle. As shown in Fig. 10(b) that the bearing capacity of pile groups significantly increases with the increase of pile number under the same pile spacing. Moreover, it should be noted that the increase in the number of piles effectively reduces the settlement of the pile foundation. When the load applied to the pile cap is 1000 kN, the settlement values of 2×2 piles, 5 piles, 3×3 piles are 35.8, 22.6, 10.3 mm, respectively. The pile foundations with a small pile number have exceeded the ultimate bearing capacity, but the 3×3 piles foundation is in the elastic stage. The above observations indicate that both the pile spacing and pile number have significant effects on the bearing performance of pile groups.

8. Conclusions

In this study, a new analytical approach for evaluating

the load-displacement response of a single tapered pile and tapered pile groups was proposed. Three analysis stages were applied in the presented method, in which the elastic and elastoplastic solutions of cavity expansion were used to evaluate the response between unit shear stress and pile displacement due to slip at the soil-pile interface, respectively. Based on the K_0-AMCC model, the initial stress anisotropy of the cohesive soil around the pile was considered. An effective iterative computer program was developed for nonlinear analysis of the load-displacement behaviour of a single tapered pile.

In an adjacent identical tapered pile analysis system, the interaction between pile shafts and interaction between pile bases were considered separately. The shaft response of the unloaded tapered pile was obtained using the FDM, and the linear elastic model was used to simulate the interaction developed at the pile base. A reduction coefficient was introduced into the discussion of pile shaft interaction to illustrate the reinforcing effect between tapered piles. Then the pile top settlement of any tapered pile in the pile groups was determined, and the settlement calculation methods of pile groups were proposed according to different pile cap stiffness. The analytical approach of tapered single pile and pile groups were validated using two 3D FE programs, respectively, considering the K_0-consolidated characteristics of soft clay. The comparison results show that reasonable predictions can be made using the method proposed in this paper. The result of the parameter study showed that the bearing capacity of tapered piles increases with the increase of taper angle, pile spacing and pile number, and significant decreases with the increase of the anisotropy of the surrounding soil. The influence of soil anisotropy on the load-displacement of the tapered piles should be considered in actual construction.

The calculated load-displacement curves are the result of a certain period after the load stabilizes and represents the short-term bearing characteristics. The change in load-bearing performance caused by the dissipation of excess pore pressure over time will be discussed in future studies.

References

Comodromos, E.M., Papadopoulou, M.C. and Rentzeperis, I.K. (2009), "Pile foundation analysis and design using experimental data and 3-D numerical analysis", *Comput. Geotech.*, **36**(5), 819-836. https://doi.org/10.1016/j.compgeo.2009.01.011.

Elias, V., Welsh, J., Warren, J., Lukas, R., Collin, G. and Berg, R.R. (2006), *Ground Improvement Methods*, *Vol. II*, FHW A-NHI-06-020, Federal Highway Administration, Washington, D.C., U.S.A.

El Naggar, M.H. and Wei, J.Q. (1999), "Axial capacity of tapered piles established from model tests", *Can. Geotech. J.*, **36**(6), 1185-1194. https://doi.org/10.1139/t99-076.

Guo W.D. and Randolph M.F. (1998), "Rationality of load transfer approach for pile analysis", *Comput. Geotech.*, **23**, 85-112. https://doi.org/10.1016/S0266-352X(98)00010-X.

Hamderi, M. (2018), "Comprehensive group pile settlement formula based on 3D finite element analyses", *Soils Found.*, **58**(1), 1-15. https://doi.org/10.1016/j.sandf.2017.11.012.

Hataf, N. and Shafaghat, A. (2015), "Optimizing the bearing capacity of tapered piles in realistic scale using 3D finite element method", *Geotech. Geol. Eng.*, **33**, 1465-1473. https://doi.org/10.1007/s10706-015-9912-6.

He, J., Liu, J., Zhang, K., Wu, Y. and Cao, Z. (2012), "Experimental study of bearing behaviour of composite foundation with rammed soil-cement tapered piles", *Chin. J. Rock Mech. Eng.*, **31**(7), 1506-1512 (in Chinese). https://doi.org/10.3969/j.issn.1000-6915.2012.07.026.

Khan, M.K., El Naggar, M.H. and Elkasabgy, M. (2008), "Compression testing and analysis of drilled concrete tapered piles in cohesive-frictional soil", *Can. Geotech. J.*, **45**(3), 377-392. https://doi.org/10.1139/T07-107.

Kodikara, J., Kong, K.H. and Haque, A. (2006), "Numerical evaluation of side resistance of tapered piles in mudstone", *Géotechnique*, **56**, 505-510. https://doi.org/10.1680/geot.56.7.505.

Kodikara, J.K. and Moore, I.D. (1993), "Axial response of tapered piles in cohesive frictional ground", *J. Geotech. Eng.*, **119**, 675-693. https://doi.org/10.1061/(ASCE)0733-9410(1993)119:4(675).

Kurian, N.P. and Srinivas, M.S. (1995), "Studies on the behaviour of axially loaded tapered piles by the finite element method", *Int. J. Numer. Anal. Met.*, **19**, 869-888. https://doi.org/10.1002/nag.1610191204.

Lee, C.Y. (1993), "Settlement of pile group-practical approach", *J. Geotech. Eng.*, **119**(9), 1449-1461. https://doi.org/10.1061/(ASCE)0733-9410(1993)119:9(1449).

Lee, K.M. and Xiao, Z.R. (2001), "A simplified method for nonlinear analysis of single piles in multilayered soils", *Can. Geotech. J.*, **38**(5), 1063-1080. https://doi.org/10.1139/t01-034.

Li, C. and Zou, J.F. (2019), "Created cavity expansion solution in anisotropic and drained condition based on Cam-Clay model", *Geomech. Eng.*, **19**(2), 141-151. http://doi.org/10.12989/gae.2019.19.2.141.

Li, C., Zou, J.F. and Li, L. (2019), "Elasto-plastic solution for cavity expansion problem in anisotropic and drained soil mass", *Geomech. Eng.*, **19**(6), 513-522. http://doi.org/10.12989/gae.2019.19.6.513.

Li, L., Chen, H., Li, J. and Sun, D. (2021), "An elastoplastic solution to undrained expansion of a cylindrical cavity in SANICLAY under plane stress condition", *Comput. Geotech.*, **132**, 103990. https://doi.org/10.1016/j.compgeo.2020.103990.

Li, L., Li, J. and Sun, D. (2016), "Anisotropically elasto-plastic solution to undrained cylindrical cavity expansion in K_0-consolidated clay", *Comput. Geotech.*, **73**, 83-90. https://doi.org/10.1016/j.compgeo.2015.11.022.

Li, L., Li, J., Sun, D. and Gong, W. (2017a), "A semi-analytical approach for time-dependent load-settlement response of a jacked pile in clay strata", *Can. Geotech. J.*, **54**(12), 1682-1692. https://doi.org/10.1139/cgj-2016-0561.

Li L., Li J., Sun, D. and Gong, W. (2017b), "Analysis of time-dependent bearing capacity of a driven pile in clayey soils by total stress method", *Int. J. Geomech.*, **17**(7), 04016156. https://doi.org/10.1061/(ASCE)GM.1943-5622.0000860.

Li, L., Li, J., Wang, Y. and Gong, W. (2020), "Analysis of nonlinear load-displacement behaviour of pile groups in clay considering installation effects", *Soils Found.*, **60**(4), 1-15. https://doi.org/10.1016/j.sandf.2020.04.008.

Liu, J., He, J. and Min, C. (2010), "Contrast research of bearing behavior for composite foundation with tapered piles and cylindrical piles", *Rock Soil Mech.*, **31**(7), 2202-2206. https://doi.org/10.16285/j.rsm.2010.07.027 (in Chinese).

Liu, J., He, J., Wu, Y. and Yang, Q. (2012), "Load transfer behaviour of a tapered rigid pile", *Géotechnique*, **62**, 649-652. https://doi.org/10.1680/geot.11.T.001.

Manandhar, S. and Yasufuku, N. (2012), "Analytical model for the end bearing capacity of tapered piles using cavity expansion theory", *Adv. Civ. Eng.*, 339-347. https://doi.org/10.1155/2012/749540.

Manandhar, S. and Yasufuku, N. (2013), "Vertical bearing capacity of tapered piles in sands using cavity expansion theory", *Soils*

Found., **53**, 853-867. https://doi.org/10.1016/j.sandf.2013.10.005.
Mayne, P.W., and Kulhawy, F.H. (1982), "K0-OCR relationships in soils", *J. Geotech. Eng.*, **108**(6), 851-872. https://doi.org/10.1016/0148-9062(83)91623-6.
Mylonakis, G., and Gazetas, G. (1998), "Settlement and additional internal forces of grouped piles in layered soil", *Géotechnique*, **48**(1), 55-72. https://doi.org/10.1680/geot.1998.48.1.55.
Paik, K., Lee, J. and Kim, D. (2011), "Axial response and bearing capacity of tapered piles in sandy soil", *Geotech. Test. J.*, **34**, 1-9. https://doi.org/10.1520/GTJ102761.
Paik, K., Lee, J. and Kim, D. (2013), "Calculation of the axial bearing capacity of tapered bored piles", *Proc. ICE Geotech. Eng.*, **166**(5), 502-514. https://doi.org/10.1680/geng.10.00127.
Randolph, M.F. and Wroth, C.P. (1978), "Analysis of deformation of vertically loaded piles", *J. Geotech. Geoenviron. Eng.*, **104**, 1465-1488. https://doi.org/10.1061/AJGEB6.0000729.
Randolph, M.F. and Wroth, C.P. (1979), "An analysis of the vertical deformation of pile groups", *Géotechnique*, **29**(4), 423-439. https://doi.org/10.1680/geot.1979.29.4.423.
Sakr, M., and El Naggar, M.H. (2003), "Centrifuge modeling of tapered piles in sand", *Geotech. Test. J.*, **26**(1), 22-35. https://doi.org/10.1520/GTJ11106J.
Singh, S. and Patra, N.R. (2020), "Axial behavior of tapered piles using cavity expansion theory", *Acta Geotech.*, **15**, 1619-1636. https://doi.org/10.1007/s11440-019-00866-y.
Wang, Z., Xie, X. and Wang, J. (2012), "A new nonlinear method for vertical settlement prediction of a single pile and pile groups in layered soils", *Comput. Geotech.*, **45**, 118-126. https://doi.org/10.1016/j.compgeo.2012.05.011.
Wei, J. and El Naggar, M.H. (1998), "Experimental study of axial behaviour of tapered piles", *Can. Geotech. J.*, **35**(4), 641-654. https://doi.org/10.1139/cgj-35-4-641.
Yang, C., Chen, H. and Li, J. (2020), "Drained cylindrical cavity expansion analysis in anisotropic soils considering 3D strength" *Géotechnique Lett.*, **10**(2), 346-352. https://doi.org/10.1680/jgele.19.00043.
Yang, C., Li, J., Li, L. and Sun, D. (2021), "Expansion responses of a cylindrical cavity in overconsolidated unsaturated soils: A semi-analytical elastoplastic solution", *Comput. Geotech.*, **130**, 103922. https://doi.org/10.1016/j.compgeo.2020.103922.
Zhang, Q. and Zhang, Z. (2012), "Simplified calculation approach for settlement of single pile and pile Groups", *J. Comput. Civ. Eng.*, **26**(6), 750-758. https://doi.org/10.1061/(ASCE)CP.1943-5487.0000167.
Zil'berberg, S.D. and Sherstnev, A.D. (1990), "Construction of compaction tapered pile foundations", *Soil Mech. Found. Eng.*, **27**(3), 96-101. https://doi.org/10.1007/BF02306664.

CC